EFFECT OF IMPURITY DOPING CONCENTRATION ON SOLAR CELL OUTPUT

P. A. Iles and S. I. Soclof

Optical Coating Laboratory Inc., Photoelectronics Group
Industry, California

SUMMARY

Experimental measurements were made of solar cell and related photovoltaic parameters for silicon with high concentrations of dopant impurities. The cell output peaked for doping levels around 10^{17} cm^{-3}. Independent measurements of diffusion length and open circuit voltage at high doping levels showed severe reductions at concentrations above 10^{17} to 10^{18} cm^{-3}. Theoretical reasons are given to explain these reductions. Indication is given of the problems requiring solution before increased cell output can be achieved at high doping levels.

INTRODUCTION

To date, silicon solar cell power conversion efficiency as a function of doping level has generally peaked in the 10^{16} cm^{-3} doping range (1). Lower doping concentrations gave slightly higher short circuit current (Isc) because of increased diffusion length, with lower open circuit voltage (Voc), and therefore lower output. Addition of a back surface field to the cell structure (1-3) allowed combination of the high Isc resulting from lower doping levels, and Voc comparable to values obtained from doping levels around 10^{16} cm^{-3}. Recently, significantly higher values of Isc have been obtained by increasing the response at short wavelengths, as in the violet cell (4), and by the further overall increase in response given by the non-reflective form of the violet cell (5).

Calculations show that the Isc and curve fill factor (CFF) values presently obtained for these advanced cells are approaching the maximum obtainable; therefore further significant increases in silicon solar cell output must be obtained by increase in Voc. Theoretically, increased Voc should be obtained at higher doping levels, because of the greater separation of Fermi levels in the N and P regions.

DEPENDENCE OF CELL OUTPUT ON SILICON DOPING

Solar cells were made (by conventional processing) from a number of single crystal silicon ingots covering a wide range of impurity concentrations (10^{13} to 10^{20} cm^{-3}).

Figure 1 shows the maximum power obtained at various doping levels; Pmax is seen to reach a maximum at doping levels around 10^{17} cm^{-3}. Figure 2 shows the breakdown of the three photovoltaic parameters which determine Pmax (Isc, Voc, CFF), over the same doping range. All three parameters decrease severely for concentrations exceeding 10^{17} cm^{-3}.

Separate measurements of diffusion length (L) and Voc were made on a variety of silicon cells (or diodes) extending over the same wide doping range (6,7).

Figure 3 shows L versus doping concentration; L is high for low doping levels, with wide spread, because of varying degrees of crystalline perfection. For N above $10^{17}cm^{-3}$, L decreases rapidly and the measured spread is reduced.

Figure 4 shows the calculated photocurrent density versus concentration; Jsc was calculated using the L-values in Figure 3.

Figure 5 shows the dependence of minority carrier lifetime (τ) on N, derived from Figure 3, using concentration dependent mobility values (8).

Figure 6 shows Voc versus N. Voc is low for lightly doped silicon, reaches a peak around 10^{18} cm^{-3}, and then decreases rapidly for doping concentrations above 10^{18} cm^{-3}.

Figure 7 plots output power density as a function of doping, combining the Voc variations in Figure 6 with the Jsc variations in Figure 4, and assuming plausible CFF values. Even with ideal Voc behavior, the decrease in Jsc dominates the power output.

THEORETICAL CONSIDERATIONS

The theoretical causes underlying these high doping concentration results were studied, to explain the experimental results, and also to indicate how further increases in cell output might be obtained.

Diffusion Length Versus Concentration

The experimental fall-off of L for doping concentrations above $10^{17}cm^{-3}$ could be caused by:

(a) Non-intentional inclusion (with the doping sources) of larger concentrations of "killer" impurities (such as iron, gold, copper, etc.)

(b) Carrier trapping caused by the intentional dopants, resulting from recombination

via the unionized shallow impurity levels (9). Although such shallow traps probably have low capture cross sections, their high concentration could result in significant carrier capture.

Another carrier loss mechanism dependent on the high dopant concentrations could be band-to-band Auger recombination (10,11).

Either mechanism would result in approximately inverse square dependence of carrier lifetime on doping density at high doping levels; the experimental curve (Figure 5) has a slope around -1.7 close to the inverse square case. If the cause of L-decrease is (a) above, there are experimental possibilities for reducing the killer impurity levels. However if the intentional dopants and/or the Auger recombination mechanism are the main cause of L-decrease, there is small prospect of maintaining high Isc values at high doping concentrations.

Open Circuit Voltage Versus Concentration

Simple PN junction theory predicts a steady decrease of diode saturation current (and therefore increased Voc) with higher doping concentrations (12, 13). However, closer study has identified several independent mechanisms which can severely increase diode excess currents at high doping levels. These mechanisms include:

(a) Reverse injection from the bulk silicon into the thin, highly doped diffused layer, aided by band gap narrowing in the diffused layer (7, 14-16).

Figure 8 shows the calculated variation of Voc with N, for simple diode theory, then plotted using the corrected parameters, and finally allowing for band gap narrowing effects. The theoretical curve is seen to approach the experimental curve.

(b) The effect of low carrier lifetimes in the PN junction depletion region. At high doping levels, this depletion region is very narrow (less than $0.1 \mu m$), and very short carrier lifetimes can be expected in this location. Using plausible values for the low and high lifetime values occurring in the depletion region, it was possible to simulate the unilluminated forward-biased I-V diode characteristics measured for a wide range of high doping levels. Often the slope of the ln I-V characteristics was around 1.75, for up to four decades of current, in a region where two separate exponential diode characteristics are usually assumed.

(c) The high overall dopant concentration may lead to precipitates or crystallographic imperfections which can promote internal shunt paths, reducing junction voltage.

FUTURE PROSPECTS

Higher Efficiency Cells

Present practical work is aimed at finding structures or processes which can reduce the high doping effects discussed in the previous section, and which will increase output from cells made from highly doped silicon.

Many of the methods already successful in achieving high Isc, namely surface texturing, increased active area, and improved antireflective coatings, are usable for low resistivity silicon.

There may be several serious problems in achieving high output with highly doped silicon.

(a) Good quality shallow PN junctions may be difficult to achieve because the reduced surface concentrations will not overdope the highly doped bulk sufficiently, and the high total impurity concentration may increase the incidence of precipitates, with increased chance of shunting of the PN junction. Also the higher vacancy density resulting from the high doping density may complicate the control of shallow diffusions.

(b) There may be difficulties in maintaining high Isc values because the diffusion length may be reduced both by the lower bulk silicon perfection resulting from the high doping levels, and also because of the carrier capture and recombination mechanisms discussed.

(c) Voc can be maximized only by selecting the initial doping concentration, and the junction formation methods to minimize the combined effects of reverse injection, low lifetime in the bulk and depletion regions, and band gap narrowing.

(d) The formation of adequate back surface fields will be more difficult because of the difficulty in providing back surface dopant concentrations significantly higher than the already high bulk concentration.

To overcome these limitations, more complex cell designs, such as epitaxial structures, may be needed. Already epitaxial cell structures were made wherein the thickness of the epitaxial layer was decreased systematically, with only small increase of Voc (7). Recent theoretical calculations offer hope of increased Voc from epitaxial solar cells (17).

Lower Cost Cells

Many of the above factors must be considered in evaluating the possible output

from lower cost cells. However, there are additional factors probably present in such cells which require reconsideration of the impurity factors:

(a) The use of lower cost silicon to form the starting silicon will probably result in increased concentrations of both "killer" impurities and conventional dopants, particularly boron and aluminum.

(b) The silicon may have lower crystal perfection, probably including grain boundaries. These grain boundaries can trap charge carriers (reducing Isc), and also can increase the junction excess currents with reduced Voc and CFF. Use of higher doping levels may restrict the collection effects of the grain boundaries by reducing the extent of the depletion region surrounding the boundary.

The analysis of cell performance when such silicon is used must include previous experience for single crystal silicon, combined with increased understanding of the detailed effects of grain boundaries and impurities, and their interaction (18). In principle, some remedial experimental measures are possible to improve the performance of cells made from lower cost silicon.

CONCLUSIONS

There are serious problems in achieving significantly higher output for solar cells made from highly doped silicon. More work is needed to investigate whether some of the restrictive mechanisms discussed above can be minimized. The optimum doping level for polycrystal cells may be somewhat higher than that for single crystals.

REFERENCES

1. P. A. Iles, Proceedings of 8th Photovoltaic Specialists' Conference (1970), p. 345.
2. R. Gereth et al., Proceedings of 8th Photovoltaic Specialists' Conference (1970), p. 353.
3. J. Mandelkorn and J. Lamneck Jr., Proceedings of 9th Photovoltaic Specialists' Conference (1972), p. 66.
4. J. Lindmayer and J. F. Allison, COMSAT Tech. Rev., Vol. 3, (1973), p. 1.
5. J. Haynos et al., Proceedings of Photovoltaic Power Generation (1974), p. 487.
6. Final Report, Contract NAS 3-15689, "Effects of Processing on the Carrier Lifetime in Silicon Solar Cells," Centralab Semiconductor.
7. Final Report, Contract NAS 3-17360, "Junction Effects in Silicon Solar Cells," Centralab Semiconductor.
8. J. C. Irvin, Bell System Tech. J., Vol. 41, (1962), p. 387.
9. R. J. Whittier and J. P. Downing, "Simple Physical Model for the Injection Efficiency of Diffused PN Junctions," Paper 12.4 at 14th Int. Electron Dev. Conference (1968).
10. J. S. Blakemore, "Semiconductor Statistics" Pergamon Press.
11. W. W. Sheng, IEEE Trans. on Electron Dev., Vol. ED-22, (1975), p. 25.
12. W. Shockley, Bell System Tech. J., Vol. 28, (1949), p. 435.
13. C. T. Sah, R. N. Noyce, and W. Shockley, Proc. IRE, Vol. 45, (1957), p. 1228.
14. A. A. Vol'fson and V. K. Subashiev, Sov. Phys.--Semiconductors, Vol 1., (1967), p. 327.
15. R. Van Overstreaten, H. DeMan, and R. Mertens, IEEE Trans. on Electron Dev., Vol. ED-20, (1973), p. 290.
16. R. B. Fair, IEEE Trans. on Electron Dev., Vol. ED-20, (1973), p. 642.
17. V. L. Dalai, H. Kressel, and P. H. Robinson, J. Appl. Phys., Vol. 46, (1975), p. 1283.
18. S. I. Soclof and P. A. Iles, "Grain Boundary and Impurity Effects in Low Cost Silicon Solar Cells," these proceedings.

ACKNOWLEDGEMENTS

The authors wish to thank NASA-Lewis Research Center for contract support for much of the work described above.

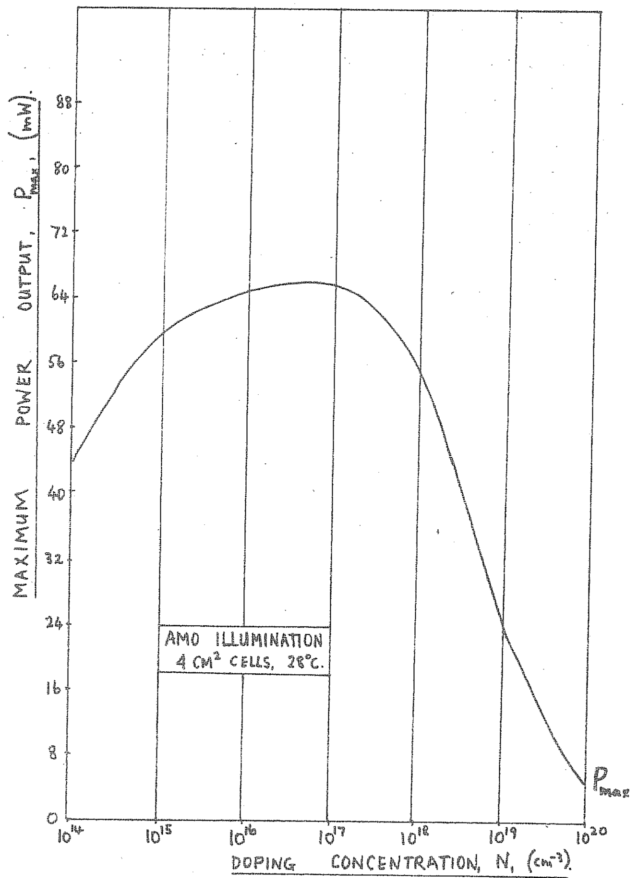

FIGURE 1 MAXIMUM CELL POWER OUTPUT OBTAINED AT VARIOUS DOPING CONCENTRATIONS; CONVENTIONAL PROCESSING.

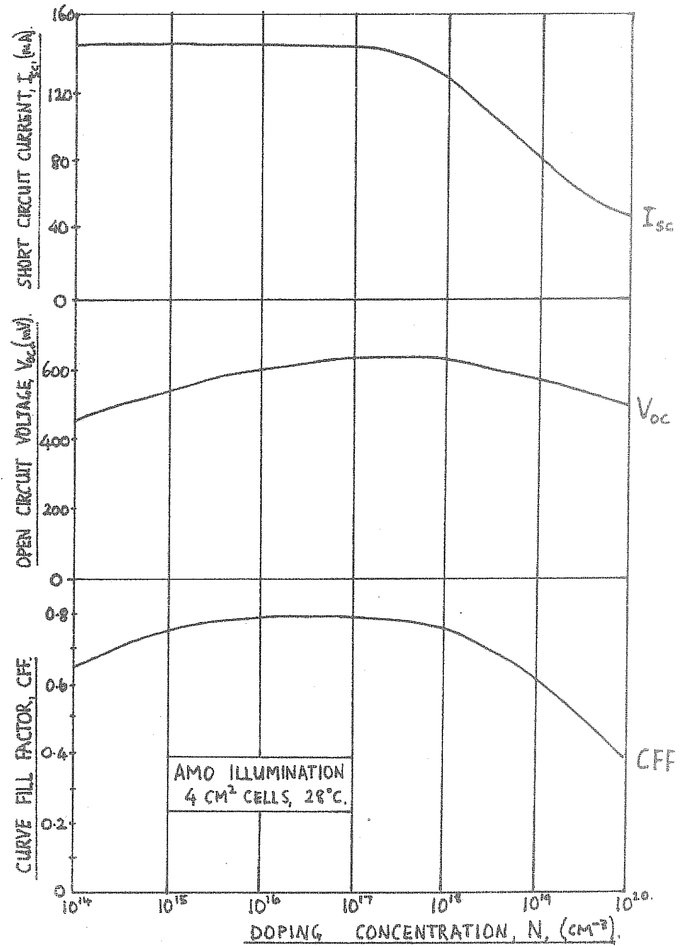

FIGURE 2 BREAKDOWN OF THREE PHOTOVOLTAIC PARAMETERS (Isc, Voc, CFF) OBTAINED AT VARIOUS DOPING CONCENTRATIONS.

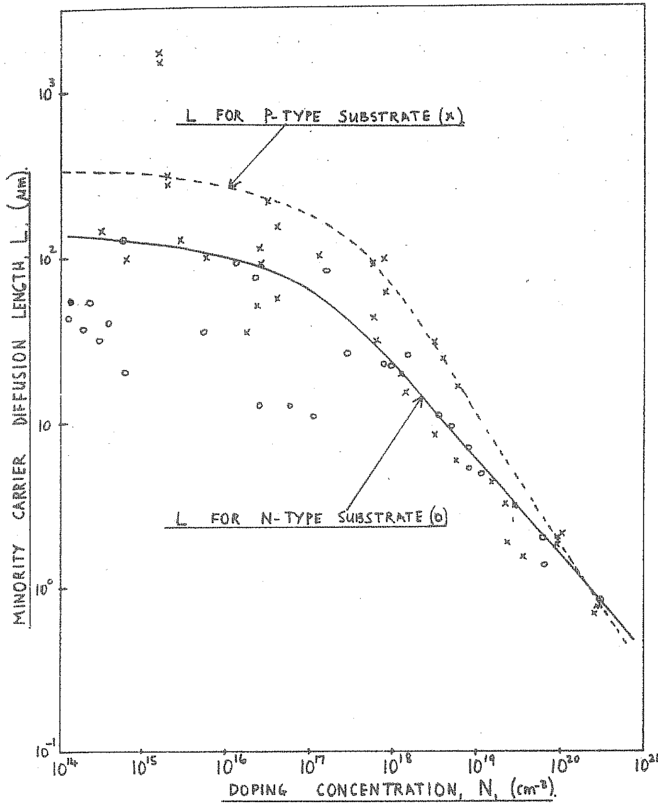

FIGURE 3 MEASURED DIFFUSION LENGTHS AS A FUNCTION OF DOPING CONCENTRATION.

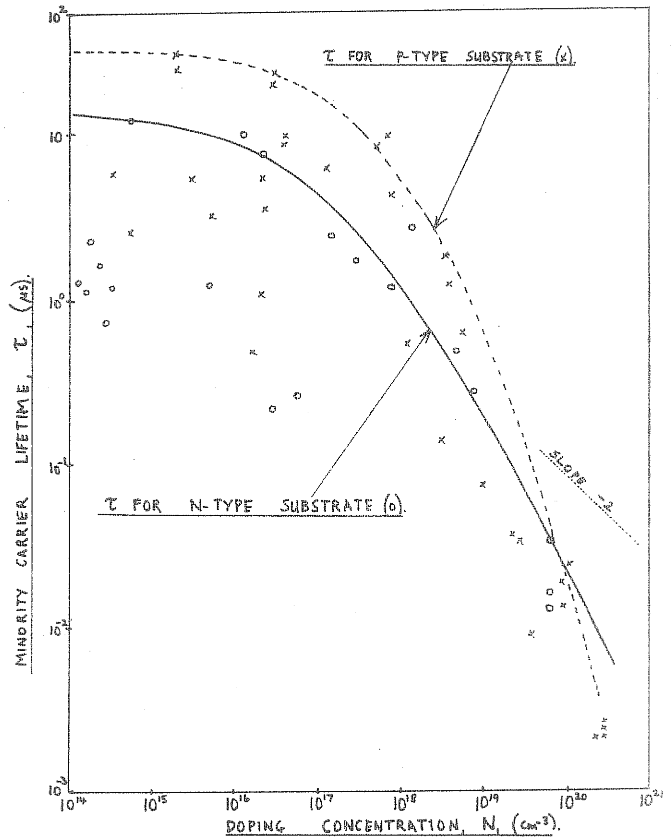

FIGURE 5 MEASURED MINORITY CARRIER LIFETIME AS A FUNCTION OF DOPANT CONCENTRATION.

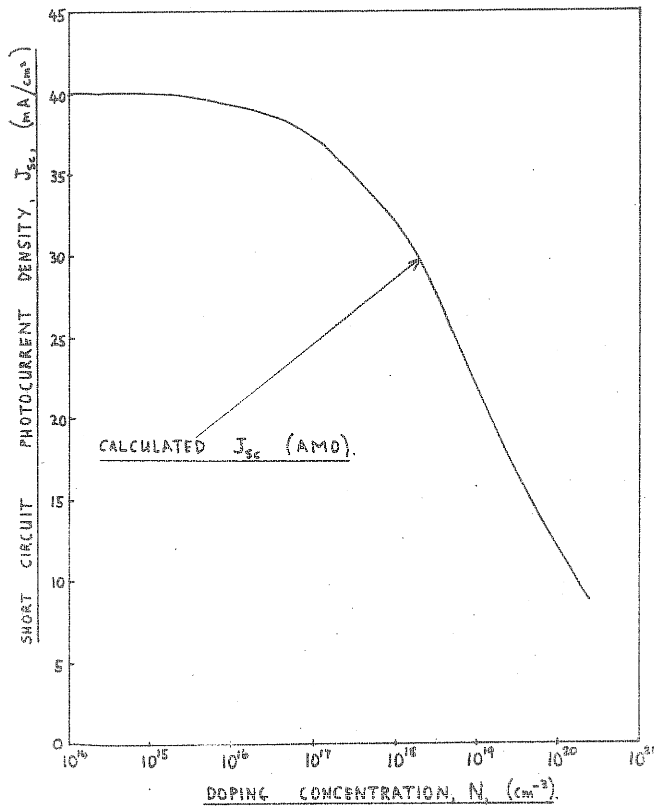

FIGURE 4 CALCULATED PHOTOCURRENT DENSITY VERSUS IMPURITY CONCENTRATION.

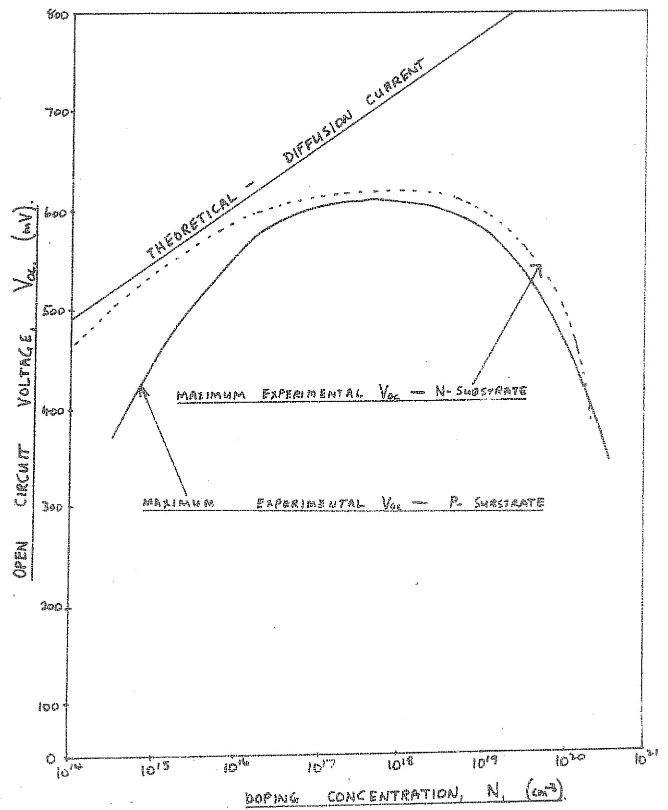

FIGURE 6 MEASURED OPEN CIRCUIT VOLTAGE VERSUS DOPING CONCENTRATION.

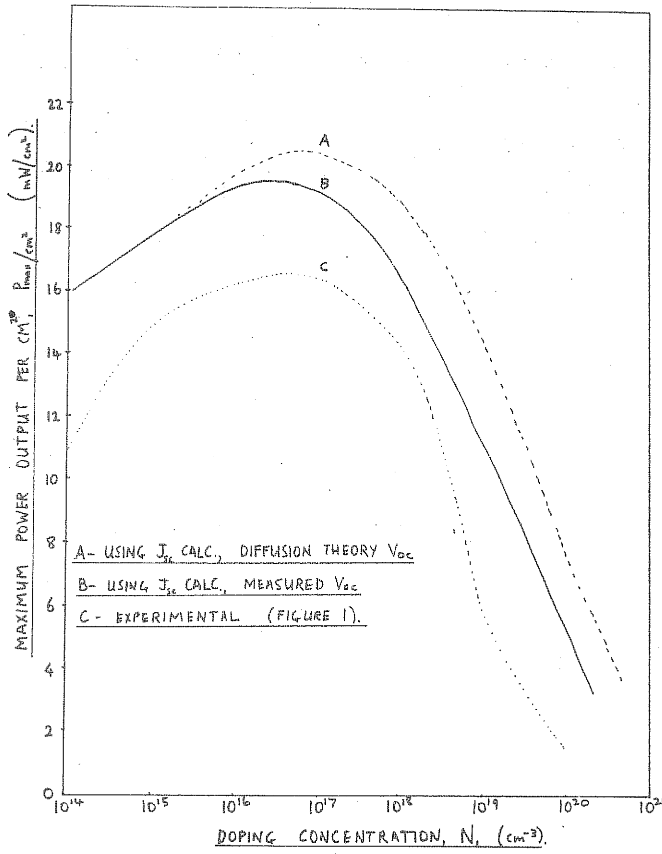

FIGURE 7 CALCULATED OUTPUT POWER DENSITY AS A FUNCTION OF DOPING.

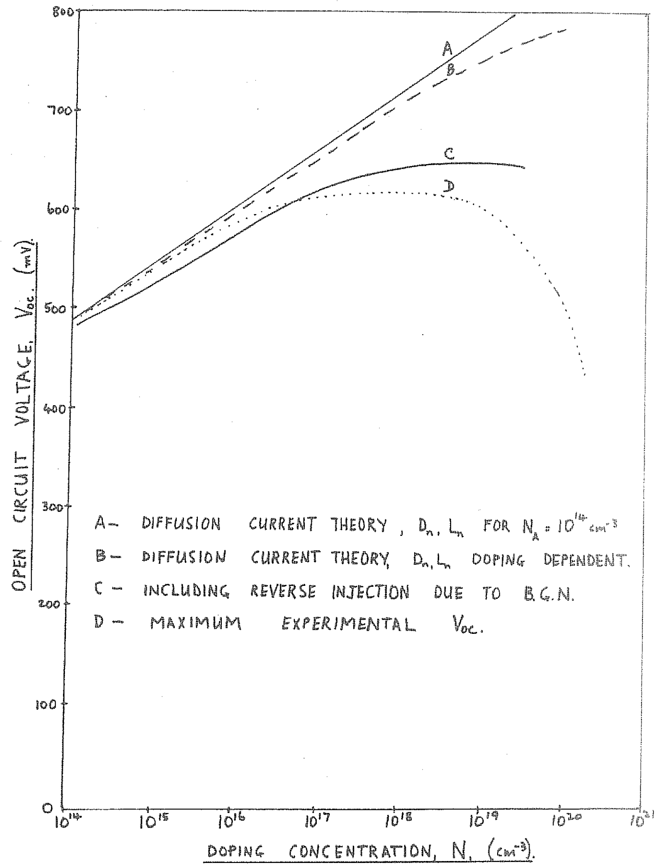

FIGURE 8 CALCULATED VARIATIONS OF OPEN CIRCUIT VOLTAGE WITH DOPANT CONCENTRATION, FOR DIFFERENT THEORETICAL CASES.